A New Fuzzy SVM based on the Posterior Probability Weighting Membership

Yan Wei*, Xiao Wu
College of Computer and Information Science, Chongqing Normal University, Chongqing, China
Email: weiyan@cqnu.edu.cn , wuxiao1985@sina.com

***Abstract*—To solve the sensitivity to the noises and outliers in support vector machine (SVM), the characterizations of fuzzy support vector machine (FSVM) are analyzed. But the determination of fuzzy membership is a difficulty. By the inspiration of bayesian decision theory and combining with sample density to give weight for each sample, new fuzzy membership function is proposed. Each sample points is given the tightness arranged forecasts by this method and the generalization ability of FSVM is improved. Numerical experiments show that, compared with the traditional SVM and FSVM, the improved algorithm performs, more effectively and accurately, has better classification result.**

***Index Terms*—Fuzzy Support Vector Machine, posterior probability, sample density, weighted membership**

I. INTRODUCTION

Support vector machine (SVM) is a powerful machine learning method calling for training data sample independent and identically distributed. It does not need any distribution information and all samples are treated fairly. But in practical applications, due to the existence of abnormal data and noise data for each sample of pollution, the influence of division to each sample should be different [1]. Fuzzy support vector machine (FSVM) is to solve this kind of problem with uncertainty.

Fuzzy support vector machine theory needs to choose the appropriate membership according to actual situation. Taiwan scholars Liu Fu Chun etc. [2] proposed the typical FSVM method based on class center distance and class attribute sample membership tectonic methods; Han-Pang Huang etc. [3] defined a linear function membership function where samples based on distance between the clustering center; Tang Hao etc. [4] combined with *k* neighboring method considering the ideas are presented to the categories of sample points for each center distance and sample points close degree arranged the estimates of subordinate function structure method; Zhang Ying etc. [5] proposed based on support vector data fields describe fuzzy membership function model, with the sample points to minimum contain super ball feature space centre distance to determine its membership. These membership function structural methods are all based on the distance and the uncertainty of sample do not consider actual fully [6-8]. By the bayesian decision theory of inspiration, in [9], by using a posterior probability to express the uncertainty of samples, Gaowei Wu etc. established a posterior probability support vector machine system framework and get a new optimization problems.

Actually, in FSVM, the membership of samples is required not only objectively and accurately to reflect the system of the uncertainty of samples, but also to describe the sample points in sample concentrated position distribution relationship. Therefore, combining bayesian theory [10-12] and sample distribution density, fuzzy support vector machine samples membership functions may further improve the structure to improve the promotion of FSVM ability.

II. BAYESIAN THEORY

Statistical decision theory is one of the basic theory processing pattern classification problems. It has a practical significance to the mode analysis and the design of classification. Bayesian Decision Theory (Bayesian Decision method is to keep) is a basic method of statistical pattern recognition and it plays an important role in the traditional mode identification field.

Bayesian decision is to generate decision-making rules (or called classifier) based on the analysis of probability to data, and then apply the generation decision rules to classify new data according to the probability. It must meet the following conditions when using the Bayesian decision-making theory [10]:

1) All the relevant probability values are known;

2) The category number of the classification by decision is must certain.

Bayesian decision-making has generated a lot of decision rules methods, such as based on the minimum error rate of Bayesian decision, based on the minimum risk decision, in Bayesian limited the condition of the error rate that another kind of minimum error rate of two categories, the smallest and the biggest decision, and sequential classification method, etc. This paper will introduce simply based on the minimum error rate of Bayesian decision-making rules.

In the pattern classification problems, people often try to reduce the error of the classification, based on this requirement, the probability of the Bayesian formula, it can generate the smallest error rate classification rules, we call it based on the minimum error rate of Bayesian decision-making.

Manuscript received April 7, 2011; revised June 28, 2011; accepted July 26, 2011.

* Corresponding author.

doi:10.4304/jcp.7.6.1385-1392

Suppose that the sample point $x=(x_1,x_2,\cdots x_n)$ is a point in space of $\mathbf{R}^n$, and the classification problem has m classes which are labeled by ω_j ($j=1,2,\cdots,m$), $\omega_1,\omega_2,\cdots,\omega_m$ is dividing the space of $\mathbf{R}^n$. In the Bayesian decision-making theory, the label ω_j is a random variable. The probability of it appears $P(\omega_j)$ can be estimated from the prior knowledge, called prior probability. Because the classification of the prior probability provided information is so limited that we need to use the information of data sample x, immediately class conditional probability density function $p(x|\omega_j)$ to make decision.

By the Bayesian decision-making hypothesis, it is known of prior probability $P(\omega_j)$ and class conditional probability density function $p(x|\omega_j)$, using Bayesian formula:

$$P(\omega_j|x)=\frac{p(x|\omega_j)P(\omega_j)}{\sum_{i=1}^{m}p(x|\omega_i)P(\omega_i)} \quad (1)$$

We call conditional probability $P(\omega_j|x)$ the state of the category posterior probability. Obviously, Bayesian formula is in essence through the observation x to translate the state of the category prior probability $P(\omega_j)$ into categories of state posterior probability $P(\omega_j|x)$.

Posterior probability A reflects the prior probability of category B and the product of the probability density in all possible prior probability of category and the product of the probability density in the sum of the proportion of the posterior probability, and it is not directly proportional to the prior probability, but depend on two parameters its prior probability and probability density.

So, Bayesian decision-making rules based on the minimum error rate is:

If $P(\omega_j|x)=\max_i P(\omega_i|x)$ Then $x\in\omega_j$, $j=1,2,\cdots,m$. Its physical meaning is that the observation under the condition of vector x occurred in n dimensional space, the max one of all conditional probability of the category ω_j should be the classes which is belonging to, this can make minimum the identification decision for error rate.

Using decision rules of classification (classifier) designed by Bayesian decision theory, it has optimal performance, means the classification error of which realize in all possible classifier is the smallest, so it is often used as a standard to measure quality of other classifier design method [10]. However, Bayesian decision theory required not only the number of categories should be known , but also has a fundamental premise, was that prior probability of each category and class conditional probability density should be known as well. In fact, prior probability and class conditional probability density are hard to know in general situation.

Analysis Bayesian decision theory made by the posterior probability decision, we can find easily[11]:

1) If we have known the form of the classified category probability distribution and training data set which has been made categories, it needs to estimate the parameters of the probability distribution from the training sample set.

2) If we don't know anything about an classification category probability distribution, it has known raining data set labeled categories and the form of function, the paper will need to from the training sample set to estimately the parameters of the discrimination function.

3) If neither know anything about an classification category probability distribution, also don't know discriminent forms, only have function marking categories of training data set. It needs from the training sample set to estimate the probability distribution function parameters.

4) Only having training data set which is not labeled categories, it is often happening. This need to set the training sample clustering, and to estimate the probability distribution parameters.

5) If we are known that classified the probability distribution of the category, hence, we do not need the training sample set, using bayesian decision theory can design the optimal classifier.

III. Sample Density of Sample Concentration

A. The Concept of Sample Density

Generally, for a given data sample set, to give its accurate data distribution model, it is impossible. But, according to the general sense, the more sample points distribute around one sample point the bigger of sample distribution density in this place, vice instead.

To consider the distance between the sample points because it can reflect the role of classification by this point in a certain extent. For designing membership function just consider the distance of sample points to the kind of center is easy to appear some mistakes. As shown in figure 1.

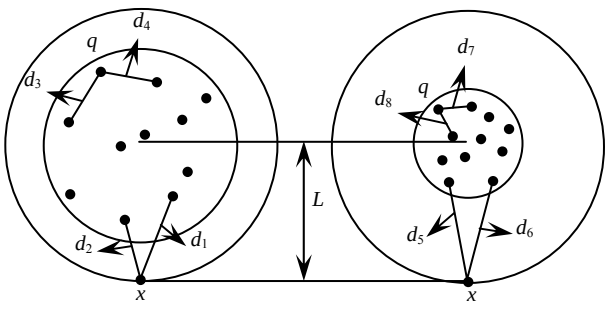

$d_1 \sim d_8$: The distance between the adjacent points

L : The distance between x and category center

Fig. 1 Different close degree of sample points

The distances between center and x are same, but the left x may very well be support vector, and the right side x may be noise points.

To sample set $T=\{(x_1,y_1),(x_2,y_2),\cdots,(x_l,y_l)\}$, $x_i\in\mathbf{R}^n$, $y_i\in\{-1,+1\}$, $i=1,2,\cdots,l$, calculate the distance between the opposite of l sample points $d_{ij}=\left\|x_i-x_j\right\|$ and form the distance matrix R of T:

$$R=\begin{bmatrix} d_{11} & d_{12} & \cdots & d_{1l} \\ d_{21} & d_{22} & \cdots & d_{2l} \\ \vdots & \vdots & \vdots & \vdots \\ d_{l1} & d_{l2} & \cdots & d_{ll} \end{bmatrix} \tag{2}$$

Then the average distance of all the sample points is:

$$D=\frac{1}{C_l^2}\sum_{i=1}^{l-1}\sum_{j=i+1}^{l}d_{ij}=\frac{2}{l(l-1)}\sum_{i=1}^{l-1}\sum_{j=i+1}^{l}d_{ij} \tag{3}$$

The maximum distance of sample points is:

$$d=\max_{i,j=1,2,\cdots,l}d_{ij} \tag{4}$$

We define the average density and samples density with average distance and maximum distance.

Definition 1[13]: Suppose n is the dimension, l is the number of the data sample set T. d is the maximum distance of all the samples in the data set, Then the average density of data sample set T is:

$$\rho=\frac{l}{t\left(\frac{\sqrt{3}}{2}\times d\right)^n} \tag{5}$$

t is constant coefficient and $t=1$ in this paper. At this time, The denominator in right of (4) means the space of multidimensional hypersphere's super "volume" of all samples in data sample set T.

If making hypersphere's diameter just with the maximum distance d of all the samples in the data set T may be due to missing some sample points, it makes that the average density can not reflect the objective situation. But after appropriate to expand scope, the closed interval would contain all the sample points and the diameter of the expanded is $\sqrt{3}$ times the original. To ensure just painted on closed interval contains all sample points in the data set from geometry[13].

In order to further distinct the position of samples in the data set, we define the density concept of the sample points. In order to bring into correspondence with the definition of the average density, in the calculation of the density of each sample point x_i ($i=1,2,\cdots,l$), we still extended the effective diameter to the original $\sqrt{3}$ times. Meanwhile, considering the samples density reflecting the sample distribution of a closed small field of sample points. Thus set λ ($0<\lambda<1$), namely the diameter of unit closed interval, is $\sqrt{3}\lambda D$. Scan data matrix R and calculate sample number of unit closed interval to each sample points l_i.

Definition 2 The average distance of sample points in the sample set T is D, set λ ($0<\lambda<1$), the sample number of distance sample point x_i less than $\sqrt{3}\lambda D/2$ is l_i. Then the density definition of sample point x_i is:

$$\rho_i=\frac{l_i}{\left(\frac{\sqrt{3}}{2}\times\lambda D\right)^n},\quad i=1,2,\cdots,l \tag{6}$$

The average density and sample density of the Sample set are similar to the definition of physics, as shown in figure 2 below.

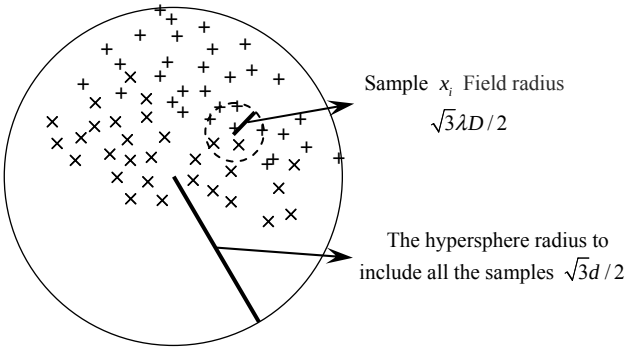

Fig. 2 Schematic of average density and sample density in sample set

The density of each sample in sample set T is defined by (5). The dense position of the sample points space relationship is reflected by the samples of different density. The dense of the sample density ρ_i ,means the more sample points adjacent sample x_i ,the role to support vector machine (SVM) of this sample is greater; The sparse of the sample density ρ_i ,means the less sample points adjacent sample x_i ,the role to support vector machine (SVM) of this sample is smaller. Usually the average density and sample density are used to outlier detection.

B. The Feature of Space Sample Density

The support vector machine in training will map the sample points of original space to feature space. When the samples of original space mapping to feature space through $\Phi(x)$, the samples of original space will resume distribution in the feature space. Because of the specific form of $\Phi(x)$ is unknown and the samples of original space about how to distribute in feature space is not know also. So it is uncertain of the noise of abnormal data (valid data) in the original space are the noise of abnormal data (valid data) in the feature space the same.

The definition of sample density mainly uses the distance between the sample points of the original space. Because the specific form of $\Phi(x)$ is unknown, the distance between the sample points in feature space can be obtained by kernel function $K(x,x')$:

$$\begin{aligned} d(\Phi(x),\Phi(x')) &= \left\|\Phi(x)-\Phi(x')\right\| = \sqrt{\langle\Phi(x)-\Phi(x'),\Phi(x)-\Phi(x')\rangle} \\ &= \sqrt{\langle\Phi(x),\Phi(x)\rangle-2\langle\Phi(x),\Phi(x')\rangle+\langle\Phi(x'),\Phi(x')\rangle} \\ &= \sqrt{K(x,x)-2K(x,x')+K(x',x')} \end{aligned} \tag{7}$$

The distance between any two sample points after mapping to the feature space can be find out through (7).

Convert d_{ij} which in R from (2) to distances of sample points in the feature space and make use of (5) and (6) to calculate, then average density and sample density of sample points will be obtained in feature space.

IV. Based on the Posterior Probability Weighted of Membership Functions

The membership function is the key to the fuzzy algorithm when to deal with the problems with fuzzy techniques. So a membership function must be able to objectively and accurately uncertainty that presents in the system. Though there are many ways to construct membership functions, currently, there is no general guidelines to follow. And in practice, we usually determine the membership function based on experience of concrete problem.

Normally, one determines the membership of samples where the basic principle is based on the relative importance in class or where the size of contribution of class in FSVM. While membership was deeply studied by many researchers, but main way is based on the distance of a sample to the centers of class, for example in [3], the membership of samples is regarded as a linear function of the distance of a sample to the centers of class. To use membership function of S function which defined by Zadeh in [10], we consider the membership and the distance are non-linear, and no longer seen as a simple linear relationship, see Ref.6. The above methods are considered by the criteria of the distance of a sample to the centers of class. When to sure membership of samples with the above methods, nevertheless, according to the methods of reducing the role of outliers of previous papers, to reduce the influence of outliers and greatly decrease performance of separating hyper-plane with SVR too, because support vectors are located at relative out-edge of two samples and the distance of samples to the centers of two samples is larger. Hence, one obtains the separating hyper-plane which is deviate from the optimal separating hyper-plane. Meanwhile, the relationship of the optimal separating hyper-plane in SVR and the center of two samples are relate with the distribution of two samples, and the distribution is unknown in advances. So, in the general case, the deviation exists. The existing membership function cannot determine membership of samples according as these methods only consider the samples in their classes, but not consider the relationship of samples and different classes.

This paper proposes a determining method of fuzzy membership based on posterior probability-weighted of two fuzzy support vector classification. On the one hand, it can reduce outliers and noise which influences the separating hyper-plane. On the other hand, it does not affect the support vector decision separating hyper-plane.

A. Confirm a Posterior Probability of Empirical Methods

With the Bayesian decision theory, we can easily determine the posterior probability of samples if we know the class prior probability and conditional probability of each sample point. In practice, however, one usually don't know the class prior probability and conditional probability of samples. With regard to the two categories FSVM, normal by using an empirical method of posterior probability[9], that is to estimate the class prior probability and conditional probability of samples based on data sample set.

Definition 3 The number of samples of class ω_j ($j=1,2$) with l_j, and $l=l_1+l_2$ is the number of samples in FSVM training sample set T. Then we can define the estimation of the class prior probability based on data sample set as follows:

$$\hat{P}(\omega_j)=\frac{l_j}{l},\quad j=1,2 \tag{8}$$

In fact, if the class prior probability of class ω_j ($j=1,2$) is P_j ($j=1,2$), the sample with independent under the condition of distribution,the probability of l_j samples belong to class ω_j in l samples is

$$P(l_j)=(l_j/l)P_j^{l_j}(1-P_j)^{l-l_j},\ j=1,2$$

The Mathematical expectation of l_j is $E(l_j)=P_jl$, and Binomial distribution in place of the mean with steep spikes , so ratio l_j/l is a very well estimates to the class prior probability.

Regard to class of conditional probability density of sample x_i, with class of conditional probability density of a small neighborhood of the input x fall into x_i sample to avoid estimate sample space distribution to replace there class of conditional probability density,in order to avoid estimating sample space distribution.

With (2) and (3), the average distance of samples in the sample set is D, D is Exist and bounded because of the number of samples l is limited. Select $0<\lambda<1$, use hypersphere

$$S(x_i,\sqrt{3}\lambda D/2)=\{x\,|\,\|x-x_i\|<\sqrt{3}\lambda D/2\}$$

To be neighborhood of x_i, as shown in figure 1 shows. Suppose the number of samples which fall into $S(x_i,\sqrt{3}\lambda D/2)$ and belongs to class ω_j ($j=1,2$) in the sample set is k_i^j.

Definition 4 To estimate of the class conditional probability of x_i in sample set T as

$$\hat{p}(x_i\,|\,\omega_j)=\frac{k_i^j}{l_j},\ j=1,2 \tag{9}$$

Then, according to Bayesian formula and the empirical estimation of the class prior probability and conditional probability density, one can obtain the posterior probability as follow:

$$P(\omega_j\,|\,x_i)=\frac{\hat{p}(x_i\,|\,\omega_j)\hat{P}(\omega_j)}{\hat{p}(x_i\,|\,\omega_1)\hat{P}(\omega_1)+\hat{p}(x_i\,|\,\omega_2)\hat{P}(\omega_2)},\quad j=1,2 \tag{10}$$

B. To Construct Membership Function based on Posterior Probability Weighted

The membership in fuzzy support vector machine mainly descript the effect level of sample point impacts

the separating hyper-plane and minimizes reduce the influence of outliers and noise to the separating hyper-plane when training support vector. Therefore, the difference of samples in different nature is based on only to present the importance of sample points in their classes with membership function but also to reflect the probability of sample points belong to which classes. With the Bayesian decision theory, the probability is decrypted by its posterior probability. We construct the membership function based on posterior probability weighted according as considering weight the posterior probability with density ratio ρ_i/ρ.

Reference [9] uses the posterior probability of samples to express the possibility of belongs to location class, combined bayesian decision-making rules and SVM, established based on the posterior probability of support vector machine. But this approach also does not consider the specific attribute at boundaryof the sample.

For a given sample data set, obviously, the more samples around a sample, the bigger sample density of this sample points, and the influence of classification is greater. On the contrary, the less samples around a sample, the smaller sample density of this sample points, and the influence of classification is smaller.

Based on the above analysis, we consider the posterior probability with density ratio ρ_i/ρ to be the weighted of reflecting the possibility of the sample belong to the class that constitutes with the based on the posterior probability weighting membership of function.

Definition 5 We define the membership function based on posterior probability weighted of x_i in sample set T as

$$\mu(x_i) = P(\omega_j \mid x_i) \bullet \left(\frac{\rho_i}{\rho}\right),\ i = 1,2,\cdots,l \tag{11}$$

In which $\mu(x_i)$ presents membership of x_i belongs to class ω_j, the posterior probability of x_i belongs to class ω_j is $P(\omega_j \mid x_i)$, and ρ or ρ_i are just mean density of sample set T or sample rate of sample point x_i, where $j = 1,2$, $i = 1,2,\cdots,l$.

In the definition 5, the possibility of posterior probability $P(\omega_j \mid x_i)$ describes the sample point x_i belonging to the class ω_j, ρ and ρ_i is the average density and sample density which is not distinguish the sample class of the whole sample set T, using ρ_i/ρ to weighted $P(\omega_j \mid x_i)$ to get the sample points of membership is based on this ideas:

1) Considering the support vector is distributed near the hyperplane, thus the sample near the hyperplane often has greater effect on classification, and we need to focus on the sample distribution position. Through ρ_i/ρ it can adjust samples in the role of classification which are near the hyperplane.

2) By the bayesian formula and the experience of posterior probability determined, $P(\omega_j \mid x_i)$ describes a small field of the local sample situation about sample point x_i in class ω_j, and the value of the size, reflecting the possibility of x_i belonging to the class ω_j. The ρ_i/ρ value reflect the sample point x_i distributs in the whole samples set T, especially samples nearby classification hyperplane , when ρ_i/ρ weighted by $P(\omega_j \mid x_i)$, give full consideration to the role of the classification.

3) In the bayesian decision-making method, if it has not good estimation about density function, the decision rules designed at last maybe not reliable. However FSVM is different from bayesian decision-making, even if we expected to receive the probability estimate accurately as possible, with the method of front experience estimates even if deviation, but Lagrange multiplier α_i in FSVM decision classification hyperplanes design can adjust the sample point x_i for classification of hyperplanes influence. At the same time, when in the estimation of conditional probability $\hat{p}(x_i \mid \omega_j)$, the field of different sample points may have cross, so total probability samples will more than 1, just $\sum_i \hat{p}(x_i \mid \omega_j) > 1$, however, such conditions probability estimate is just intermediate steps, the purpose of which is to estimate the sample points posterior probability, it does not affect the sample posterior probability estimate.

4) Because ρ is the average density of samples set T, make the value of ρ_i/ρ more than 1may also may be less than 1, when $\rho_i/\rho < 1$, that the sample point x_i is outlier or noise point has a high probability[13], at this time weighted $P(\omega_j \mid x_i)$ by ρ_i/ρ will be reduced membership value of x_i, and the role of classification is weakened, avoiding to the abnormal data monitoring and abnormal data definition membership alone . But for sample points nearby the classification hyperplane, because ρ and ρ_i is defined on the whole sample set, $P(\omega_j \mid x_i)$ is the sample estimate in the same class, so ρ_i/ρ weighted and will increase membership of these samples, which increases the role of the classification.

To set the training sample set

$$T = \{(x_1, y_1), (x_2, y_2), \cdots, (x_l, y_l)\}$$

$x_i \in \mathbf{R}^n$, $y_i \in \{-1, +1\}$, $i = 1,2,\cdots,l$, with considering the uncertain factors about outliers and noise in sample set, then re-construct sample set with FSVM as follow:

$$(x_1, y_1, \mu_1), (x_2, y_2, \mu_2), \cdots, (x_l, y_l, \mu_l) \tag{12}$$

In which y_i stands for classification status flag, $y_i = +1$ is positive class and mark ω_1 (ω_1 is +); $y_i = -1$ is negative class and mark ω_2 (ω_2 is −); So the membership can be calculated with (11) as follow.

$$\mu_i = \mu(x_i) = \begin{cases} P(+ \mid x_i) \bullet \left(\dfrac{\rho_i}{\rho}\right), & y_i = +1 \\ P(- \mid x_i) \bullet \left(\dfrac{\rho_i}{\rho}\right), & y_i = -1 \end{cases} \tag{13}$$

C. The Membership Algorithm based on Posterior Probability Weighted

The samples in feature space will be re-distribute when samples in sample space is mapped to feature space by mapping of $\Phi(x)$, then spatial relationship between samples changes, so one calculates membership in feature space with (13).

Algorithm 1 The membership algorithm based on posterior probability weighted

Input: To set the training set

$$T=\{(x_1,y_1),(x_2,y_2),\cdots,(x_l,y_l)\}$$

$x_i\in\mathbf{R}^n$, $y_i\in\{-1,+1\}$, $i=1,2,\cdots,l$, where $0<\lambda<1$.

Output: To set the membership of sample x_i , where $i=1,2,\cdots,l$.

Step 1: To create the distance matrix R of sample set T with (7), to calculate the average distance D and the largest distance d of sample set with (3) and (4).

Step 2: To calculate the average density ρ of sample set.

Step 3: To calculate priori class probability $\hat{P}(+)$ and $\hat{P}(-)$ with (8) according as y_i in T .

Step 4: To research x_i in sample set T , where $i=1,2,\cdots,l$

{

1) To scan distance matrix R , to calculate the number of samples l_i which the distance of R to x_i is less than $\sqrt{3}\lambda D/2$ and the number of samples k_i^j which similar with y_i .

2) To calculate the density ρ_i of sample point x_i with (6).

3) When $y_i=+1$,To compute conditional class probability $\hat{p}(x_i\mid -)$ or posterior probability $P(-\mid x_i)$ of x_i , and with (9) or (10).

4) To calculate μ_i with (13) and ρ , ρ_i , $P(+\mid x_i)$ (or $P(-\mid x_i)$).

}

The membership algorithm 1 based on posterior probability weighted is end when one compute membership of all samples in T , the time complexity is $O(l^2)$ where the member of samples is l in T and the time consuming mainly in calculating the distance between sample points and researching distance matrix.

V. WEIGHTED FSVM BASED ON THE POSTERIOR PROBABILITY

The core idea of fuzzy support vector machine (FSVM) is the introduction fuzzy membership, according to different input data to the classification with the different contribution, given the corresponding membership, which is weighted the sample by the membership functions, extends traditional SVM soft interval algorithm to solve uncertainty classification problem [2,14,15]. This can reduce the effect of outlier and noise, improving the SVM classification performance.

Given the training sample set T :

$$T=\{(x_1,y_1,\mu_1),(x_2,y_2,\mu_2),\cdots,(x_l,y_l,\mu_l)\} \quad (14)$$

Where $x_i\in\mathbf{R}^n$ is sample characteristic, $y_i\in\{-1,+1\}$ is category label, μ_i indicate the degree of x_i belonged to y_i , we call it the membership of sample (x_i,y_i,μ_i) for $i=1,2,\cdots,l$.

For obtaining the good promotion ability of the fuzzy support vector machine (SVM) ,we also needs to maximize classification interval and minimizing errors, and it is different from the penalty factor of traditional support vector machine (SVM), being considered that reduce the influence of sample points which is not important, fuzzy support vector machine with the training sample of membership fuzzy the penalty factor. We can ensure the membership of training sample by the weighted the samples posterior probability of the sample characteristics to determine by the type (13) , then fuzzy support vector machine solution the optimal hyperplanes for the optimization problem is[2]:

$$\begin{aligned}\min_{w,\xi}\quad & \frac{1}{2}\|w\|^2+C\sum_{i=1}^{l}\mu_i\xi_i\\ \text{s.t.}\quad & y_i(w\cdot\Phi(x_i)+b)\geq 1-\xi_i,\quad i=1,2,\cdots,l\\ & \xi_i\geq 0,\quad i=1,2,\cdots,l\end{aligned} \quad (15)$$

Using the sample A membership weighted posterior probability, it can certain reduce the influence of relaxation variables B in FSVM in extent. At the same time affected the corresponding input data x_i the role of FSVM: μ_i smaller, the corresponding input data x_i role in the classification of hyper planes will be lower, and it also reaches according to certain rules on the importance of input data classification purpose, reduces the influence of outlier and noise, and improves the ability of SVM classification.

Construct the Lagrange function[2]

$$\begin{aligned}L(w,b,\xi,\alpha,\beta)=&\frac{1}{2}\|w\|^2+C\sum_{i=1}^{l}\mu_i\xi_i-\\ &\sum_{i=1}^{l}\alpha_i\left[y_i((w\cdot\Phi(x_i))+b)-1+\xi_i\right]-\sum_{i=1}^{l}\beta_i\xi_i\end{aligned} \quad (16)$$

Where α and β are non-negative Lagrange multipliers, according to the Wolfe dual definition,

We get Lagrange function tiny about w , b and ξ_i , by the KKT condition:

$$\frac{\partial}{\partial w}L(w,b,\xi,\alpha,\beta)=w-\sum_{i=1}^{l}\alpha_i y_i\Phi(x_i)=0$$

$$\frac{\partial}{\partial b}L(w,b,\xi,\alpha,\beta)=-\sum_{i=1}^{l}\alpha_i y_i=0$$

$$\frac{\partial}{\partial \xi_i}L(w,b,\xi,\alpha,\beta)=C\mu_i-\alpha_i-\beta_i=0$$

Generation into Lagrange function type (16), eliminating Lagrange multiplier β , we can get the dual problem of optimization problem (15):

$$\begin{aligned} \min \quad & \frac{1}{2}\sum_{i=1}^{l}\sum_{j=1}^{l}\alpha_i\alpha_j y_i y_j K(x_i,x_j)-\sum_{i=1}^{l}\alpha_i \\ \text{s.t.} \quad & \sum_{i=1}^{l}\alpha_i y_i = 0 \\ & 0 \le \alpha_i \le \mu_i C, \quad i=1,2,\cdots,l \end{aligned} \tag{17}$$

Where $C>0$ is penalty parameter, indicate the punishment degree of right sample points which is wrong classification, $K(x_i,x_j)=(\Phi(x_i)\bullet\Phi(x_j))$ is the kernel function which is meet Mercer theorem.

Solving quadratic optimization problem (17), and get the optimal FSVM classification hyperplanes decision function:

$$f(x)=\operatorname{sgn}\left(\sum_{i=1}^{l}\alpha_i^* y_i K(x,x_i)+b^*\right) \tag{18}$$

Where $b^*=y_j-\sum_{i=1}^{l}\alpha_i^* y_i K(x_i,x_j)$, subscript $j\in\{j\mid 0<\alpha_j^*<\mu_j C\}$.

Obviously, the only difference between the fuzzy support vector machine and the traditional support vector machine (SVM) is the upper bound of Lagrange multipliers α_i in the dual problem. In traditional support vector machine, the upper bound of α_i is constant C, and the upper bound α_i of fuzzy support vector machine (SVM) is the dynamic bound contain membership functions, sample points belong to the class membership is lower, the feasible region of α_i is smaller.

VI. Experimental Results

A. Data Sample Obtain

This section will be done the simulation experiment that FSVM weighted fuzzy membership based on the posterior probability application, and a example to verify the effectiveness of the improvement performance.

In order to validate the performance of based on the posterior probability weighted membership function FSVM, we use double helix line samples and the SPECT Heart Data Set from UCI machine learning database to conduct an experiment.

1) Double helix line samples

The way to produce samples of the double helix line:

angle=(i* π)/(16*density);

radius=maxRadius*((104*density-i)/(104*density));

x=radius*cos(angle); y=radius*sin(angle); //first spiral line

x=(-radius*cos(angle)-0.5);y=(-radius*sin(angle)-0.5); //second spiral line

As shown in figure 3 shows only 50 sample points.

The sample set is:

Data1: set maxRadius=3, density=1,i=1 to 100. Two spirals produced 200 sample points, each spiral get 66 samples as the training sample set, the rest samples are used to be test sample set.

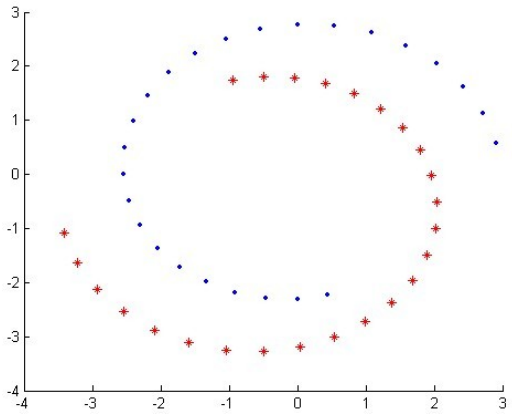

Fig. 3 Double helix line samples

2) SPECT Heart Data Set

The SPECT heart data set is a single proton computer tomography heart data set through the launch in the UCI machine learning database, to determine the heart is normal or not. SPECT Heart data set contain 267 samples, 80 among them used for the training samples, the last 187 used for test samples. In fact SPECT Heart data set is divided into two subsets: SPECT Heart data subset and SPECTF Heart data subset. Thus sample sets are as follows:

Data2: SPECT Heart Data subset.

Each sample points have 23 attributes, among them the second to 23rd attributes value is 0 or 1 of sample points of features, are with heart related properties. Attribute 1 for each sample point is the class attribute, decides the category of sample point belongs to. Where the value is 1 says the sample points for normal, value is 0 says the sample points for not normal.

Data3: SPECTF Heart Data subset.

Each sample points have 45 attributes, among them the second to 45th attributes value is 50-90 of sample points of features, are with heart related properties. Attribute 1 for each sample point is the class attribute, decides the category of sample point belongs to. Where the value is 1 says the sample points for normal, value is 0 says the sample points for not normal.

B. Simulation Experiment

Respectively, with C-SVM, based on distance defined by membership function FSVM[3] and based on the posterior probability weighting membership of fuzzy support vector machine in this paper to Data1, Data2 and Data3 training learning, gets the corresponding classification decision-making function. Punish coefficient $C=50$,adopt Gauss RBF kernel function as kernel function. Use the corresponding decision classification function test samples for testing, gets different classification accuracy of test samples is such as table 1.

TABLE 1. Accuracy compare of three support vector classification

SVM algorithm	Data Set	Training set positive class samples	Training set negative class samples	Test set positive class samples	Test set negative class samples	Positive class Testing precision/%	Negative class Testing precision/%	Testing precision /%
C -SVM	Data1	66	66	34	34	100	50	75
Linear function FSVM[3]	Data1	66	66	34	34	100	50	75
This paper FSVM	Data1	66	66	34	34	55.88	100	77.94
C -SVM	Data2	40	40	172	15	57.56	33.33	55.61
Linear function FSVM[3]	Data2	40	40	172	15	48.26	66.67	49.73
This paper FSVM	Data2	40	40	172	15	79.07	60	77.54
C -SVM	Data3	40	40	172	15	49.42	53.33	49.73
Linear function FSVM[3]	Data3	40	40	172	15	63.37	46.67	62.03
This paper FSVM	Data3	40	40	172	15	69.19	53.33	67.91

VII. CONCLUSIONS

Inspired by the bayesian formula, we transform the membership of FSVM through posterior probability and weighted. It can be seen through the simulation experiment in the same data set based on the posterior probability weighting membership of fuzzy support vector machine in this paper and it is better than *C* -SVM and Linear function FSVM[3] in classification accuracy. Meanwhile, it also shows a good classification ability at different Data set.

ACKNOWLEDGMENT

Project supported by Scientific Research Foundation of the Chongqing Municipal Education Commission, China (No.KJ090823 and KJ110629).

REFERENCES

[1] Gu Ya-xiang, Ding Shi-fei, "Advances of Support Vector Machine", *Computer Science*, vol. 38, no. 2, pp. 14-17, 2011.
[2] C. F. Lin, S. D. Wang, "Fuzzy Support Vector Machines", *IEEE Transactions on Neural Networks*, vol.13, no. 2, pp. 464-471, 2002.
[3] H. P. Huang, Y. H. Liu, "Fuzzy Support Vector Machines for Pattern Recognition and Data Mining", *International Journal of Fuzzy Systems*, vol.4, no. 3, pp. 826-835, 2002.
[4] Hao Tang, Yuhe Liao, Feng Sun, Xie Hang, "The FSVM Algorithm with Fuzzy Membership", *Journal of Xi'an Jiaotong University*, vol.43, no.7, pp. 40-43, 2009.
[5] Ying Zhang, Hongye Sun, Jian Zhu, "Fuzzy Support Vector Regression Based on Data Domain Description", *Journal of Information and Control*, vol. 34, no. 1, pp. 1-6, 2005.
[6] Hsu Che-Chang, Han Ming-Feng, Chang Shih-Hsing, Chung Hung-Yuan, "Fuzzy support vector machines with the uncertainty of parameter C", *Expert Systems with Applications*, vol. 36, Issue 3, pp. 6654-6658, 2009.
[7] Li Miao-miao, Xiang Feng-hong, Liu Xin-wang, "A Novel Membership Function for Fuzzy Support Vector Machines", *Computer Engineering & Science*, vol. 31, no. 9, pp. 92-94, 2009.
[8] Li Lei, Zhou Meng-meng, Lu Yan-ling, "Fuzzy Support Vector Machine Based on Density with Dual Membership", *Computer Technology and Development*, vol.19, no. 12, pp. 44-46, 2009.
[9] Gaowei Wu, Qin Tao, Yu Wang, "Support Vector Machines Based on Posterior Probability", *Journal of Computer Research and Development*, vol. 42, no. 2, pp. 196-202, 2005.
[10] Zhaoqi Bian, Xuegong Zhang, *Pattern Recognition* (*Second Edition*), Beijing: Tsinghua University Press, 2000.
[11] Mengcehng Yao, *Probability and Statistics Tutorial*, Beijing: Tsinghua University Press, 2007.
[12] Yong Zhang, Zhong-Xian Chi, "A Fuzzy support vector classifier based on Bayesian optimization", *Fuzzy Optim Decis Making*, vol. 7, pp. 75–86, 2008.
[13] Huaji Shi, Shuyong Zhou, Xingyi Li, Hui Tang, Qiulin Ding, "To Detect Outlier Based on the Average Density", *Journal of University of Electronic Science and Technology of China*, vol. 36, no. 6, pp. 1286-1288, 2007.
[14] Hao Tang, Liang-sheng Qu, "Fuzzy support vector machine with a new fuzzy membership function for pattern classification", *Proceedings of the Seventh International Conference on Machine Learning and Cybernetics*, pp. 768-773, 2008.
[15] Nemmour Hassiba, Chibani Youcef, "Fuzzy integral to speed up support vector machines training for pattern classification", *International Journal of Knowledge Based Intelligent Engineering Systems*, vol. 14, Issue 3, pp. 127-138, 2010.

Yan Wei male, 1970-12-10 born in Sichuan China, In 1994, Chongqing Normal College mathematics education profession undergraduate course graduation won the bachelor's degree, In 2001, Chongqing University computer software and theory of the professional graduate student to master degree, In 2010, Chongqing University control theory and control engineering in the graduate student holding doctor degree. Research direction: Machine learning and intelligent computing, support vector machine theory and algorithm.

He is vice president of the college of computer and information science in Chongqing Normal University. Published paper more than 30 piece in computer simulation, computer science etc., at present, have interest in fuzzy support vector machine learning algorithm and kernel method.

He is Chongqing university young and middle-aged backbone teachers, the national normal higher school education research association, director of artificial intelligence academic committee of Chongqing, YOCSEF (CCF Young Computer Scientists & Engineers Forum) Chongqing AC members.

Xiao Wu male, 1985-12-27 born in Hubei China, Master graduate student, Research direction: machine learning and intelligent computation.

doi:10.4304/jcp.7.6.1392-1399

Research on Under-actuated Flexible Pectoral Fin of Labriform Fish

Qiang Liu
School of Electronic Engineering, Huaihai Institute of Technology, Lianyungang, P. R. China
School of Communication and Control Engineer, Jiangnan University, Wuxi, P. R. China
E-mail: qiangliu0007@163.com

***Abstract*—The new propulsor, whose inspiration is from pectoral fins of fishes, has arisen increasing attention. To improve the performance of the existing labriform bionic pectoral fin, based on the structure and control mechanism of real fish pectoral fin, the under-actuated technology was utilized to design a new flexible bionic pectoral fin. Then, the kinematic model of pectoral fin during fish forward steady swimming and the dynamic model of bionic pectoral was built. Finally, Matlab was used to simulate the kinematic and dynamic performance of bionic pectoral fin. The simulation result shows that the new flexible bionic pectoral fin can imitate the propulsion motion morphology of pectoral fin during fish forward steady swimming well. However, due to the restriction of kinematic model of pectoral fin and structure as well as physical properties of bionic fin ray, there is still tolerance between the locomotion morphology of bionic pectoral fin and that of real fish. Therefore, it is necessary to develop further research on kinematic modeling of pectoral fin and bionic design of fin ray. Additionally, the new bionic pectoral fin reduces the number of the driving variables, providing the possibility and the basis of further reducing the volume as well as the complexity of bionic device of pectoral fin.**

***Index Terms*—Flexible pectoral fin; Under-actuated; Labriform mode; Mathematical model**

I. INTRODUCTION

Labriform Mode is an important maneuvering locomotion mode which is largely applied to teleost fish [1]. It takes the pectoral fin as the main maneuvering surface, accomplishing a variety of maneuvering locomotion such as hovering, forward-swimming, backward-swimming, braking and turning. These maneuvering performances with high-efficiency and flexibility are absent in the conventional underwater vehicle [2]. To improve the maneuvering performance of underwater vehicle so as to satisfy the demands in the exploration of marine resource and protection of marine environment, the new propulsor, whose inspiration is from pectoral fins of fishes, has arisen increasing attention [2,3].

For the exploration of new maneuvering surface of underwater vehicles, study on bionic pectoral fin is of great theoretical and practical significance. However, research on anatomical structure, neuromuscular control, physical properties of fin surface and otherwise reveals that the structure and control of fish pectoral fin is extremely precise and complex, and the pectoral fin also has numerous freedoms [4-9]. Therefore, building a set of system, which can imitate the locomotion morphology of fish pectoral fin precisely, is difficult and challenging. Fig.1 is the skeleton structure of pectoral fin of labriform fish. J.Palmisano et al [10,11] built the bionic fin ray according to the structural and physical properties of fin rays and installed the fin rays on the fin base(viz. scapula, coracoid, radial bones, cartilage pad and so on) in line. Under the driving of electromotor, active deformation of the fin rays arose, with which the fin surface also became deformed. Then, the flapping locomotion of the whole fin surface was achieved by electromotor driving the fin base.

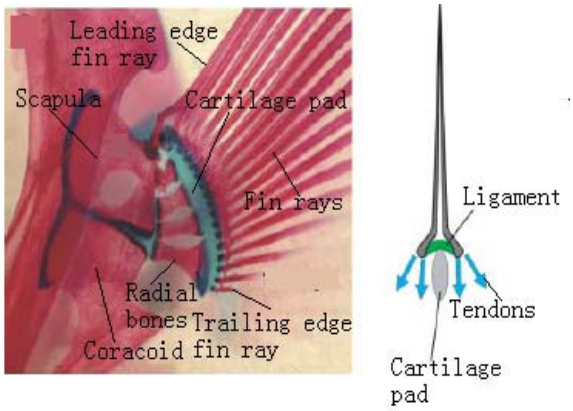

Fig.1 Skeleton structure of pectoral fin

G.V.Lauder and J.L.Tangorra et al [3,12] built the bionic fin ray according to the structural and physical properties of fin ray, then the elastic material was utilized to build the bionic fin base. Since the fin base is elastic and flexible, the bionic pectoral fin can achieve four kinds of single locomotion morphology such as expansion, curling, sweeping and cupping easily by the drive of nylon rope. The complex locomotion pattern could be created by superimposing combinations of other three single locomotion pattern onto sweep motion. J.L.Tangorra and J.R.Gottlieb et al [13, 14] combined the flexible fin rays together according to the shape of fin base, of which each fin ray can achieve the rotation motion of two freedoms. Additionally, the nylon rope driven by the electromotor was used to control the rotation motion of fin rays with the aim of achieving all kinds of propulsion locomotion of pectoral fin. However, the freedoms of this bionic pectoral fin are numerous, its structure is also very complex and its complexity

increases rapidly with the number of fin rays. In conclusion, the research on bionic pectoral fin is still insufficient. It is difficult for the present bionic pectoral fin to achieve all kinds of complex maneuvering locomotion as well as to be applied to underwater vehicles. Therefore, the research on the design of new flexible bionic pectoral fin based on the structure of fish pectoral fin and the neuromuscular control mechanism is of extreme significance.

Based on the skeleton structure and the neuromuscular control mechanism of fish pectoral fin, a new under-actuated flexible bionic pectoral fin was designed by utilizing the leading action of the leading edge fin ray and the trailing edge fin ray. Its kinematic and dynamic models were built. Then Matlab was used to simulate the locomotion morphology and performance of flexible bionic pectoral fin. Finally, the comparing analysis validated the rationality and effectiveness of the bionic pectoral fin.

II. STRUCTURE AND MOTION CHARACTERISTIC OF PECTORAL FIN

According to the skeleton structure of pectoral fin shown in Fig.1, the pectoral fin mainly consists of fin base and fin ray. The fin base plays an important role in supporting the fin ray. All fin rays are bilaminar except the leading edge fin ray, which are two curved half rays termed hemitrichs, and each end of hemitrichs is attached with tendon. Under the contraction and stretch of the muscle of both sides, the fin rays can not only achieve lateral rotation as shown in Fig.2(b) but also produce deformation which can change the shape and stiffness of the fin surface. Moreover, the fin rays can also achieve dorsal-ventral rotation as shown in Fig.2(a) under the action of muscle bundles as well as membranes between fin rays, but they mainly rotate towards the side of the trailing edge fin ray. The rotation motion towards the side of the leading edge fin ray is mainly led by the leading edge fin ray[15]. Through the rotation motion of fin rays on the two freedoms, the fish achieves various maneuvering locomotion such as propulsion, turning, backward-swimming, hovering, braking and so on[5,8].

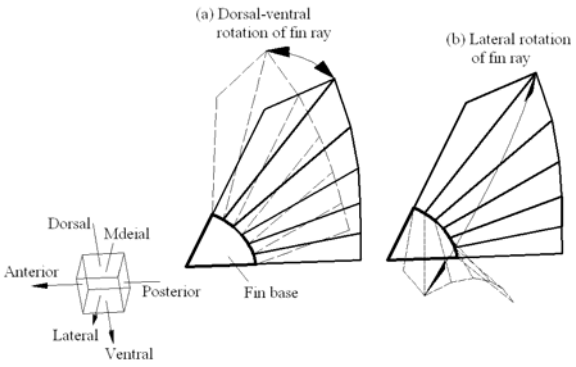

Fig.2 Two components of rotation motion of fin ray

III. DESIGN OF FLEXIBLE BIONIC PECTORAL FIN

Analysis on the skeleton structure and the neuromuscular control mechanism of pectoral fins reveals that the pectoral fin rays can achieve dorsal-ventral rotation as well as lateral rotation actively or passively under the action of muscle bundles and membranes between fin rays. Taking the complexity of muscular control into account, to reduce the difficulty in the bionic design of flexible pectoral fin, the assumption on the structure of flexible pectoral fin, motion control mechanism and physical property is described as follows:

1) Both the fin rays and fin base of pectoral fins are rigid.

2) The dorsal-ventral rotation of median fin rays is caused by the pull of leading edge fin ray and trailing edge fin ray.

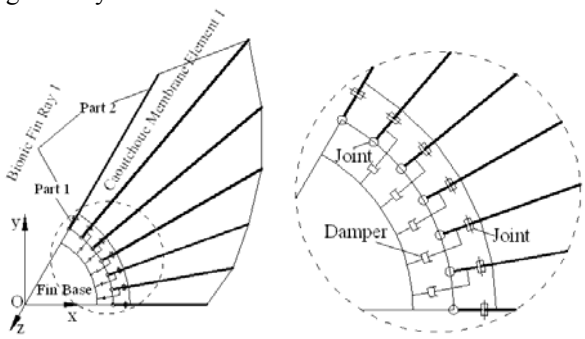

Fig.3 Schematic diagram of flexible bionic pectoral fin

The flexible bionic pectoral fin shown in Fig.3 composes of two parts(part 1 and part 2). Part 1 is actually a short link. It can swing dorsal-ventrally. Part 2 can swing laterally. Since the link is short, the bionic fin rays can imitate the swing motion of two freedoms of real fin rays well. The fin rays are connected with each other by means of caoutchouc membrane.

In addition, this paper takes the two-freedom swing of the leading edge ray and the trailing edge ray as active motion. For the median fin rays between the leading edge ray and the trailing edge ray, the dorsal-ventral swing is taken as active motion, while the lateral swing is taken as the passive motion. These motions of fin rays interact with each other by means of caoutchouc membrane. In order to reduce the oscillation of the median fin rays in the plane of fin base under the inertia force, this paper set the damping components to them.

IV. KINEMATIC MODEL OF PECTORAL FIN PROPULSION

Assume that the bionic pectoral fin area is the minimum at the initial time. For the dorsal-ventral rotation of fin rays of bionic pectoral fin, when the leading edge fin ray rotates dorsally, the fin surface expands dorsally as well. At this moment, if the trailing edge fin ray also rotates dorsally, pectoral fin with different areas and dorsal directions will be achieved. Similarly, on the condition that the trailing edge fin ray rotates ventrally, if the leading edge fin ray also rotates ventrally, thus pectoral fin with different areas and ventral

directions will be achieved as well. When the leading edge fin ray rotates dorsally while the trailing edge fin ray rotates ventrally, the surface of pectoral fin will expand towards both sides and the direction of pectoral fin will change with the rotation angle of leading edge fin ray as well as trailing edge fin ray. Therefore, the bionic pectoral fin can imitate the change of area and direction of pectoral fin during a variety of maneuvering locomotion of fish. Then, combining the above dorsal-ventral rotation motion of fin rays with the lateral rotation motion, a variety of maneuvering locomotion of pectoral fin such as hovering, forward-swimming, backward-swimming, braking and turning will be achieved. In the following analysis, the propulsion locomotion of pectoral fin during fish forward steady swimming is provided as an instance to build the kinematic model of bionic pectoral fin.

During the fish forward steady swimming, the propulsion locomotion of pectoral fin can de divided into two phases, a recovery stroke(abduction) and a power stroke (adduction). At the recovery stroke, the pectoral fin rays primarily move anteriorly and ventrally. At the power stroke, the pectoral fin rays primarily move posteriorly and dorsally, as is shown in figure 3. Since the amplitude of the dorsal-ventral rotation of the trailing edge fin ray is very small, this paper takes the amplitude of the dorsal-ventral rotation of trailing edge fin ray as zero. Thus the mathematic models of the dorsal-ventral rotation of the leading edge fin ray as well as the lateral rotation of all fin rays are built as follows [16].

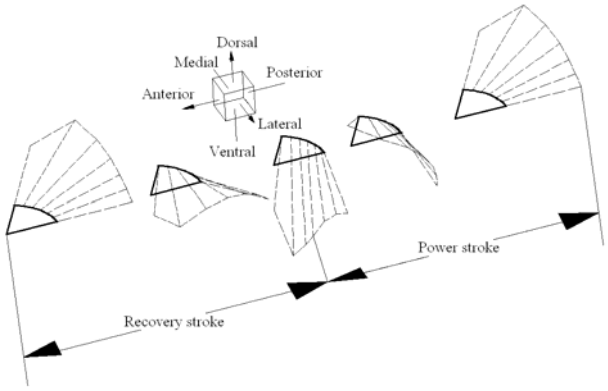

Fig.4 3D motion morphology of pectoral fin during fish forward steady swimming

Recovery stroke:

$$ {}^{1}\theta_1 = \frac{{}^{1}\widetilde{\theta}_1}{2}\left[1-\cos(\pi t / T_r)\right] \quad (0 \le t \le T_r) \tag{1} $$

$$ {}^{i}\theta_2 = \begin{cases} 0, & (\pi + {}^{i}\overline{\theta}_2)t / T_r \le {}^{i}\overline{\theta}_2) \\ \dfrac{{}^{i}\widetilde{\theta}_2}{2}\left\{1-\cos\left[\dfrac{(\pi+{}^{i}\overline{\theta}_2)t}{T_r} - {}^{i}\overline{\theta}_2\right]\right\}, & (\pi+{}^{i}\overline{\theta}_2)t/T_r > {}^{i}\overline{\theta}_2) \end{cases} \quad (0 \le t \le T_r, i = 1 \sim 7) \tag{2} $$

Power stroke:

$$ {}^{1}\theta_1 = \frac{{}^{1}\widetilde{\theta}_1}{2}\left[1+\cos(\pi t / T_r)\right] \quad (T_r \le t \le T) \tag{3} $$

$$ {}^{i}\theta_2 = \begin{cases} {}^{i}\widetilde{\theta}_2, & (\pi + {}^{i}\overline{\theta}_2)(t-T_r)/T_p \le {}^{i}\overline{\theta}_2) \\ \dfrac{{}^{i}\widetilde{\theta}_2}{2}\left\{1+\cos\left[\dfrac{(\pi+{}^{i}\overline{\theta}_2)(t-T_r)}{T_p} - {}^{i}\overline{\theta}_2\right]\right\}, & (\pi+{}^{i}\overline{\theta}_2)(t-T_r)/T_p > {}^{i}\overline{\theta}_2) \end{cases} \quad (T_r \le t \le T, i = 1 \sim 7) \tag{4} $$

where ${}^{1}\theta_1$ is the dorsal-ventral rotation angle of the leading edge fin ray; ${}^{i}\theta_2$ is the lateral rotation angle of the i th fin ray; ${}^{1}\widetilde{\theta}_1$ is the dorsal-ventral rotation amplitude of the leading edge fin ray; ${}^{i}\widetilde{\theta}_2$ is the lateral rotation amplitude of the i th fin ray; ${}^{i}\overline{\theta}_2$ is the phase delay of lateral rotation of the i th fin ray, it increases evenly from the fin ray 1 with $0°$ to the fin ray 7; T_r, T_P and T indicate the duration time of the recovery stroke, the duration time of the power stroke and the propulsion locomotion period of pectoral fin respectively.

V. MATHEMATICAL MODEL OF FLEXIBLE BIONIC PECTORAL FIN

As shown in Fig.4, the bionic pectoral fin is the rigid-flexible coupling system which is composed of fin base, two-link bionic fin ray and caoutchouc membrane element. Moreover, there is also complex coupling between pectoral fin and fluid during the propulsion locomotion of pectoral fin. Therefore, it is extremely complex and difficult to build a precise dynamic model of pectoral fin. For the sake of simplicity, neglect the mass of the caoutchouc membrane element as well as its deformation under the force of fluid. Besides, we assume that the caoutchouc membrane element is pure elastic element only affording pull force, and deformation of the caoutchouc membrane element along the length of fin ray and the thickness of fin surface under the pull of fin ray is neglected. In addition, assume that the fluid force to which the fin ray is subjected primarily results from the fluid force acted on the bilateral caoutchouc membrane elements of fin ray. Based on the above assumption, the following dynamic model of flexible bionic pectoral fin is built.

A. Dynamic Model of Bionic Pectoral Fin

For the i th two-link bionic fin ray, the dynamic model based on Lagrange method can be defined as.

$$\frac{d}{dt}\left(\frac{\partial {}^{i}T}{\partial {}^{i}\dot{\theta}_j}\right)-\frac{\partial {}^{i}T}{\partial {}^{i}\theta_j}={}^{i}Q_j \qquad (i=1\sim 7,\ j=1\sim 2) \qquad (5)$$

Where, ${}^{i}\theta_j$ and ${}^{i}\dot{\theta}_j$ are the j th generalized coordinate and generalized velocity of the i th two-link bionic fin ray respectively; t is time; ${}^{i}T$ is the kinetic energy of the i th bionic fin ray; ${}^{i}Q_j$ is the generalized force acted on the i th bionic fin ray corresponding to the j th generalized coordinate; i is the serial number of the two-link bionic fin ray; j is the serial number of the part of two-link bionic fin ray.

The kinetic energy ${}^{i}T$ of the i th two-link bionic fin ray can be defined as:

$$\begin{aligned}{}^{i}T=&\frac{1}{2}{}^{i}m_1\,{}^{i}V_{c1}^2+\frac{1}{2}{}^{i}m_2\,{}^{i}V_{c2}^2+\frac{1}{2}{}^{i}J_{c1}\,{}^{i}\dot{\theta}_1^2\\&+\frac{1}{2}{}^{i}J_{c2}({}^{i}\dot{\theta}_1^2+{}^{i}\dot{\theta}_2^2) \qquad (i=1\sim 7)\end{aligned} \qquad (6)$$

Where ${}^{i}V_{c1}^2={}^{i}\dot{x}_{c1}^2+{}^{i}\dot{y}_{c1}^2+{}^{i}\dot{z}_{c1}^2$;

${}^{i}V_{c2}^2={}^{i}\dot{x}_{c2}^2+{}^{i}\dot{y}_{c2}^2+{}^{i}\dot{z}_{c2}^2$;

${}^{i}\dot{x}_{c1}=-{}^{i}l_{c1}\sin({}^{i}\theta_{10}+{}^{i}\theta_1)\,{}^{i}\dot{\theta}_1$;

${}^{i}\dot{y}_{c1}={}^{i}l_{c1}\cos({}^{i}\theta_{10}+{}^{i}\theta_1)\,{}^{i}\dot{\theta}_1$;

${}^{i}\dot{z}_{c1}=0$;

${}^{i}\dot{x}_{c2}=-{}^{i}l_1\sin({}^{i}\theta_{10}+{}^{i}\theta_1)\,{}^{i}\dot{\theta}_1-{}^{i}l_{c2}\cos({}^{i}\theta_{10}+{}^{i}\theta_1)\sin({}^{i}\theta_{20}+{}^{i}\theta_2)\,{}^{i}\dot{\theta}_2-{}^{i}l_{c2}\sin({}^{i}\theta_{10}+{}^{i}\theta_1)\cos({}^{i}\theta_{20}+{}^{i}\theta_2)\,{}^{i}\dot{\theta}_1$;

${}^{i}\dot{y}_{c2}={}^{i}l_1\cos({}^{i}\theta_{10}+{}^{i}\theta_1)\,{}^{i}\dot{\theta}_1-{}^{i}l_{c2}\sin({}^{i}\theta_{10}+{}^{i}\theta_1)\sin({}^{i}\theta_{20}+{}^{i}\theta_2)\,{}^{i}\dot{\theta}_2+{}^{i}l_{c2}\cos({}^{i}\theta_{10}+{}^{i}\theta_1)\cos({}^{i}\theta_{20}+{}^{i}\theta_2)\,{}^{i}\dot{\theta}_1$;

${}^{i}\dot{z}_{c2}={}^{i}l_{c2}\cos({}^{i}\theta_{20}+{}^{i}\theta_2)\,{}^{i}\dot{\theta}_2$;

${}^{i}m_j$, ${}^{i}l_j$, ${}^{i}l_{cj}$, ${}^{i}J_{cj}$, ${}^{i}V_{cj}$, ${}^{i}\theta_j$, ${}^{i}\dot{\theta}_j$ and ${}^{i}\theta_{j0}$ indicate mass, length, the distance between centroid and joint, the moment of inertia, the centroid velocity, the rotation angle, the angular velocity and the initial angle of the part j of the i th two-link bionic fin ray respectively; ${}^{i}\dot{x}_{cj}$, ${}^{i}\dot{y}_{cj}$, ${}^{i}\dot{z}_{cj}$ are the x, y and z component of the centroid velocity of part j of the i th two-link bionic fin ray respectively.

The generalized force ${}^{i}Q_j$ acted on the i th bionic fin ray can be defined as:

$${}^{i}Q_j=-\sum_{k=1}^{2}{}^{i}m_k\,g\,\frac{\partial {}^{i}y_{ck}}{\partial {}^{i}\theta_k}+{}^{i}M_j^{'}+{}^{i}M_j \qquad (i=1\sim 7,\ j=1\sim 2) \qquad (7)$$

Where ${}^{i}x_{cj}$, ${}^{i}y_{cj}$, ${}^{i}z_{cj}$ are the x, y and z coordinate of the centroid of the part j of the i th two-link bionic fin ray respectively; g is the acceleration of gravity; ${}^{i}M_j^{'}$ indicates the generalized force of caoutchouc membrane element as well as its surrounding fluid to the i th two-link bionic fin ray; ${}^{i}M_j$ indicates the generalized force of motor(including damper) to the i th two-link bionic fin ray. ${}^{i}M_j^{'}$ can be defined as:

$$\begin{aligned}{}^{i}M_1^{'}=&\int_0^{\frac{{}^{i-1}l_2+{}^{i}l_2}{2}}({}_{i}^{i-1}\hat{F}_{x2}-{}_{i}^{i-1}F_{x2})\left[{}^{i}l_1\sin({}^{i}\theta_1+{}^{i}\theta_{10})+l\sin({}^{i}\theta_1+{}^{i}\theta_{10})\cos({}^{i}\theta_2+{}^{i}\theta_{20})\right]dl+\\&\int_0^{\frac{{}^{i}l_2+{}^{i+1}l_2}{2}}({}_{i}^{i}\hat{F}_{x2}+{}_{i}^{i}F_{x2})\left[{}^{i}l_1\sin({}^{i}\theta_1+{}^{i}\theta_{10})+l\sin({}^{i}\theta_1+{}^{i}\theta_{10})\cos({}^{i}\theta_2+{}^{i}\theta_{20})\right]dl+\\&\int_0^{\frac{{}^{i-1}l_2+{}^{i}l_2}{2}}({}_{i}^{i-1}\hat{F}_{y2}-{}_{i}^{i-1}F_{y2})\left[{}^{i}l_1\cos({}^{i}\theta_1+{}^{i}\theta_{10})+l\cos({}^{i}\theta_1+{}^{i}\theta_{10})\cos({}^{i}\theta_2+{}^{i}\theta_{20})\right]dl+\\&\int_0^{\frac{{}^{i}l_2+{}^{i+1}l_2}{2}}({}_{i}^{i}\hat{F}_{y2}+{}_{i}^{i}F_{y2})\left[{}^{i}l_1\cos({}^{i}\theta_1+{}^{i}\theta_{10})+l\cos({}^{i}\theta_1+{}^{i}\theta_{10})\cos({}^{i}\theta_2+{}^{i}\theta_{20})\right]dl\end{aligned}$$

$$\begin{aligned}{}^{i}M_2^{'}=&\int_0^{\frac{{}^{i-1}l_2+{}^{i}l_2}{2}}({}_{i}^{i-1}\hat{F}_{x2}-{}_{i}^{i-1}F_{x2})l\cos({}^{i}\theta_1+{}^{i}\theta_{10})\sin({}^{i}\theta_2+{}^{i}\theta_{20})dl+\int_0^{\frac{{}^{i}l_2+{}^{i+1}l_2}{2}}({}_{i}^{i}\hat{F}_{x2}+{}_{i}^{i}F_{x2})l\cos({}^{i}\theta_1+{}^{i}\theta_{10})\sin({}^{i}\theta_2+{}^{i}\theta_{20})dl+\\&\int_0^{\frac{{}^{i-1}l_2+{}^{i}l_2}{2}}({}_{i}^{i-1}\hat{F}_{y2}-{}_{i}^{i-1}F_{y2})l\sin({}^{i}\theta_1+{}^{i}\theta_{10})\sin({}^{i}\theta_2+{}^{i}\theta_{20})dl+\int_0^{\frac{{}^{i}l_2+{}^{i+1}l_2}{2}}({}_{i}^{i}\hat{F}_{y2}+{}_{i}^{i}F_{y2})l\sin({}^{i}\theta_1+{}^{i}\theta_{10})\sin s({}^{i}\theta_2+{}^{i}\theta_{20})dl+\\&\int_0^{\frac{{}^{i-1}l_2+{}^{i}l_2}{2}}({}_{i}^{i-1}\hat{F}_{z2}-{}_{i}^{i-1}F_{z2})l\cos({}^{i}\theta_2+{}^{i}\theta_{20})dl+\int_0^{\frac{{}^{i}l_2+{}^{i+1}l_2}{2}}({}_{i}^{i}\hat{F}_{z2}+{}_{i}^{i}F_{z2})l\cos({}^{i}\theta_2+{}^{i}\theta_{20})dl\end{aligned}$$

${}_{i}^{k}F_{x2}$, ${}_{i}^{k}F_{y2}$ and ${}_{i}^{k}F_{z2}$ $(k=i-1,i)$ indicate the x, y and z component of the elastic force acted on part 2 per unit length of the i th two-link bionic fin ray by the k th fin surface caoutchouc membrane element(viz. the fin surface element between the k th bionic fin ray and the $k+1$ th bionic fin ray), and the elastic force is zero for $k=0$ and7,.while the elastic force for $k=1\sim 6$ can be calculated by analysis on the caoutchouc membrane element; ${}_{i}^{k}\hat{F}_{x2}$, ${}_{i}^{k}\hat{F}_{y2}$ and ${}_{i}^{k}\hat{F}_{z2}$ $(k=i-1,i)$ indicate the x, y and z component of the fluid force acted on part 2 per unit length of the i th two-link bionic fin ray, and the

fluid force is zero for $k=0$ and 7, while the fluid force for $k=1\sim6$ can be got by the calculation of the fluid force acted on the caoutchouc membrane element.

Substitute Eq.(6) and Eq.(7) into Eq.(5), the dynamic model of flexible bionic pectoral fin can be described as:

$$\begin{cases} {}^{i}A_1\,{}^{i}\ddot{\theta}_1+{}^{i}A_2\,{}^{i}\theta_1\,{}^{i}\theta_2={}^{i}Q_1 \\ {}^{i}B_1\,{}^{i}\ddot{\theta}_2+{}^{i}B_2\,{}^{i}\dot{\theta}_2^2+{}^{i}B_3\,{}^{i}\dot{\theta}_1^2={}^{i}Q_2 \end{cases} \quad (i=1\sim7) \tag{8}$$

where

$${}^{i}A_1={}^{i}m_1\,{}^{i}l_{c1}^2+{}^{i}m_2\left[{}^{i}l_1+{}^{i}l_{c2}\cos({}^{i}\theta_2+{}^{i}\theta_{20})\right]^2+{}^{i}J_{c1}+{}^{i}J_{c2};$$

$${}^{i}A_2=-2{}^{i}m_2\,{}^{i}l_{c2}\sin({}^{i}\theta_2+{}^{i}\theta_{20})\left[{}^{i}l_1+{}^{i}l_{c2}\cos({}^{i}\theta_2+{}^{i}\theta_{20})\right]^2;$$

$${}^{i}B_1={}^{i}m_2\,{}^{i}l_{c2}^2\sin^2({}^{i}\theta_2+{}^{i}\theta_{20})+{}^{i}J_{c2};$$

$${}^{i}B_2=2{}^{i}m_2\,{}^{i}l_{c2}^2\sin({}^{i}\theta_2+{}^{i}\theta_{20})\cos({}^{i}\theta_2+{}^{i}\theta_{20});$$

$${}^{i}B_3={}^{i}m_2\,{}^{i}l_{c2}\sin({}^{i}\theta_2+{}^{i}\theta_{20})\left[{}^{i}l_1+{}^{i}l_{c2}\cos({}^{i}\theta_2+{}^{i}\theta_{20})\right].$$

B. Hydrodynamic Calculation

The hydrodynamic performance of flexible bionic pectoral fin, belonging to unsteady hydrodynamics, is extremely complex, and there is complex coupling between pectoral fin and its surrounding fluid. For the sake of simplicity, neglect the coupling between the caoutchouc membrane element and the fluid, and utilize a quasi-steady method to evaluate the fluid force acted on the pectoral fin[17]. Thus, the hydrodynamic force acted on the fin ray ${}^{k}_{i}\hat{F}_{x2}$, ${}^{k}_{i}\hat{F}_{y2}$ and ${}^{k}_{i}\hat{F}_{z2}$ can be calculated by the following formula.

$$\begin{bmatrix} {}^{k}_{i}\hat{F}_{x2} \\ {}^{k}_{i}\hat{F}_{y2} \\ {}^{k}_{i}\hat{F}_{z2} \end{bmatrix}=-\frac{1}{4}\rho d_{li}\left(C_n\sqrt{v_{nmx}^2+v_{nmy}^2+v_{nmz}^2}\begin{bmatrix} v_{nmx} \\ v_{nmy} \\ v_{nmz} \end{bmatrix}+C_\tau\sqrt{v_{\tau mx}^2+v_{\tau my}^2+v_{\tau mz}^2}\begin{bmatrix} v_{\tau mx} \\ v_{\tau my} \\ v_{\tau mz} \end{bmatrix}\right),(k=i,i+1;i=1\sim6) \tag{9}$$

Where v_{nmx}, v_{nmy} and v_{nmz} indicate the x, y and z component of the normal velocity of the midpoint of the link line between the two points which are on part 2 of i and $i+1$th bionic fin ray respectively and both have the same distance l to the joint of part 2; $v_{\tau mx}$, $v_{\tau my}$ and $v_{\tau mz}$ indicate the x, y and z component of the tangential velocity of the aforementioned midpoint; C_n and C_τ indicate the normal and tangential resistance coefficient of fin surface respectively; d_{li} indicates the present distance between the aforementioned two points.

C. Elastic Force Calculation of Caoutchouc Membrane Element

According to the theory of elasticity, the stress and the strain of the caoutchouc membrane element are of linear relation[18]. Assume that the surface stress coefficient is σ, the elastic force of the caoutchouc membrane element acted on the fin ray ${}^{k}_{i}F_{x2}$, ${}^{k}_{i}F_{y2}$ and ${}^{k}_{i}F_{z2}$ is defined as follows:

$$\begin{bmatrix} {}^{i+1}_{i}F_{x2} \\ {}^{i+1}_{i}F_{y2} \\ {}^{i+1}_{i}F_{z2} \end{bmatrix}=-\begin{bmatrix} {}^{i}_{i}F_{x2} \\ {}^{i}_{i}F_{y2} \\ {}^{i}_{i}F_{z2} \end{bmatrix}=\begin{cases} -\sigma\dfrac{d_{li}-d_{li0}}{d_{li}}\begin{bmatrix} {}^{i+1}x_{l2}-{}^{i}x_{l2} \\ {}^{i+1}y_{l2}-{}^{i}y_{l2} \\ {}^{i+1}z_{l2}-{}^{i}z_{l2} \end{bmatrix} & d_{li}-d_{li0}>0 \\ \begin{bmatrix} 0 \\ 0 \\ 0 \end{bmatrix} & d_{li}-d_{li0}\le0 \end{cases} \quad (i=1\sim6) \tag{10}$$

Where d_{li0} indicates the initial distance between the two points which are on part 2 of i and $i+1$th bionic fin ray respectively and both have the same distance l to the joint of part 2; ${}^{i}x_{l2}$, ${}^{i}y_{l2}$ and ${}^{i}z_{l2}$ are the coordinates of the point which is on part 2 of the ith bionic fin ray and has the distance l to the joint of part 2.

D. Damper Modeling

Suppose that the damping force acted on the fin ray is only correlated with the dorsal-ventral rotation velocity of the fin ray, thus the damping moment acted on the fin ray can be defined as[19]:

$${}^{i}M_1={}^{i}b^2\,{}^{i}C\cos^2{}^{i}\theta_1\,{}^{i}\dot{\theta}_1 \quad (i=2\sim6) \tag{11}$$

Where ${}^{i}b$ is the perpendicular distance from the action point of the damping force to the axis of part 1 of the ith bionic fin ray; ${}^{i}C$ is the damping coefficient of the damper installed on the ith bionic fin ray.

VI. SIMULATION ANALYSIS

For analyzing the performance of the flexible bionic pectoral fin, MATLAB is utilized to write the corresponding simulation program. Meanwhile, assuming that the velocity U is $0.1m/s$, the surface stress coefficient σ is 0.1 MPa, the propulsion locomotion period T is 1 s, the duration time of the power stroke T_p is 0.5 s, the duration time of the recovery stroke T_r is 0.5 s, the normal fluid resistance coefficient of fin surface C_n is 1.18, the tangential fluid resistance coefficient C_τ is 0.05.

The simulation result shown in Fig.5 and Fig.6 indicates that the transient performance of the median fin rays is excellent. Therefore, it is feasible to cause the dorsal-ventral swing of the median fin rays by means of the leading edge ray and the trailing edge ray. This can also reduce the number of the driving joints and the complexity of the flexible bionic pectoral fin.

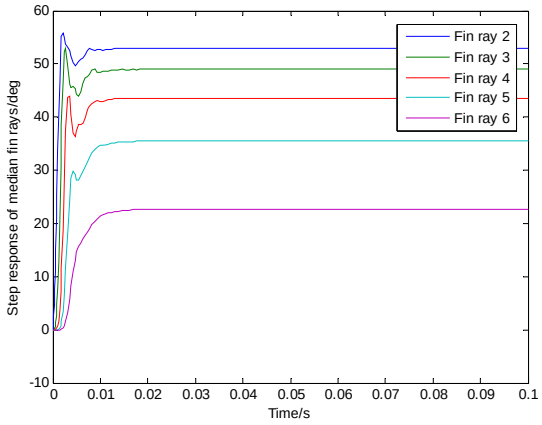

Fig.5 Step response to leading edge fin ray

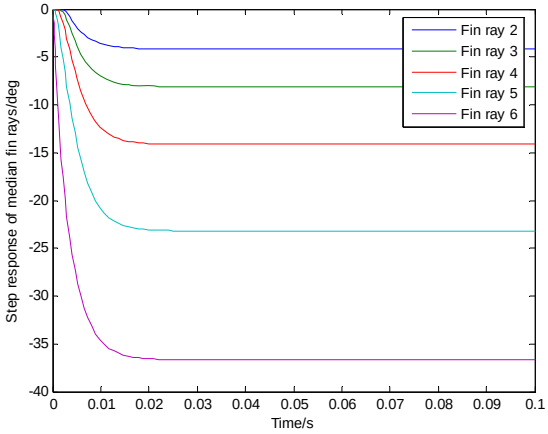

Fig.6 Step response to trailing edge fin ray

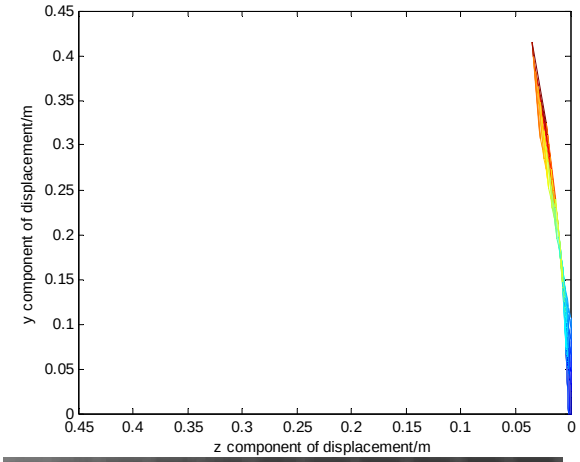

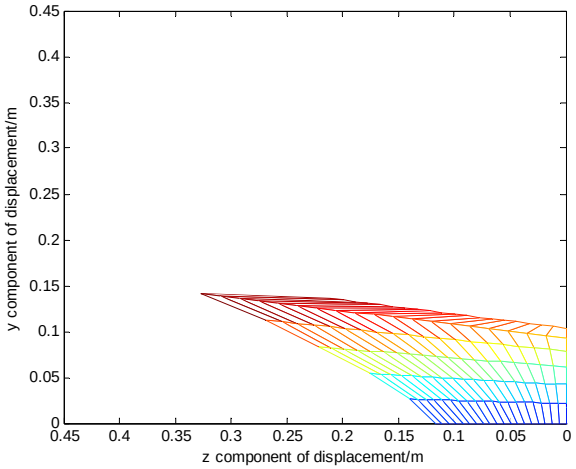

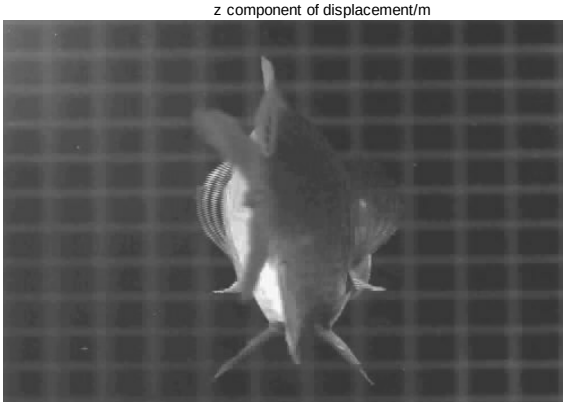

(a) $t = 0.1T$

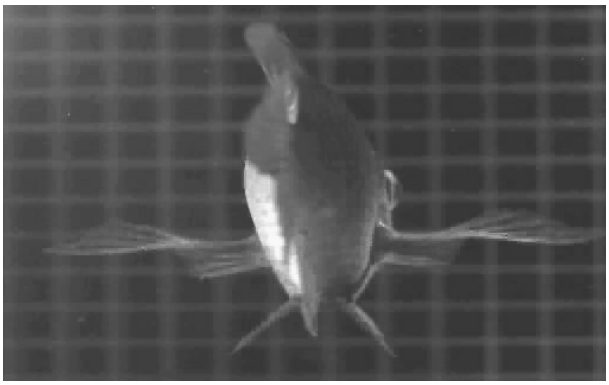

(b) $t = 0.5T$

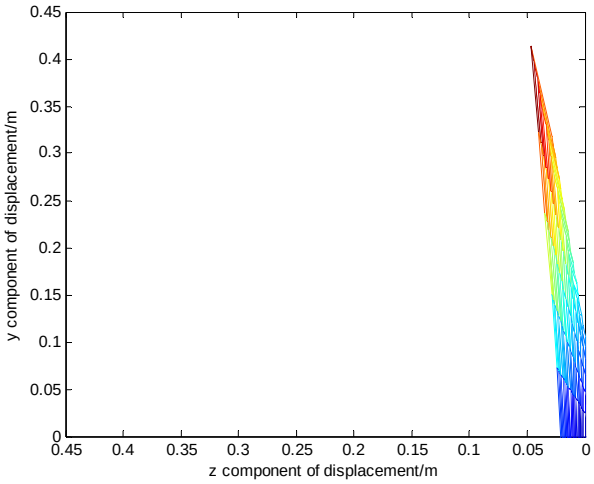

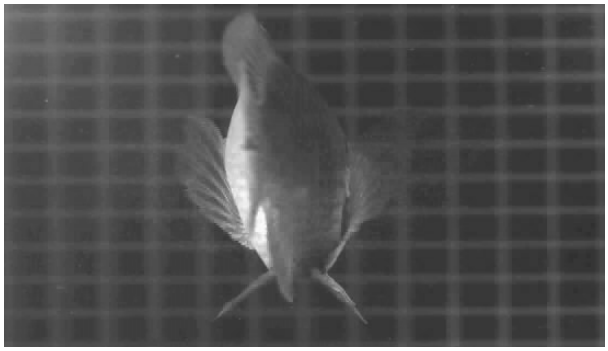

(c) $t = 0.9T$

Fig.7 Post view of propulsion morphology of bionic pectoral fin and real pectoral fin

According to he simulation result and conservation result shown in Fig.7, the new bionic system of flexible pectoral fin established in this paper can imitate the propulsion motion morphology of pectoral fin well. However, there are still some errors compared with the motion morphology of real fish pectoral fin. There are mainly two reasons for such error. On one hand, simplification is made to the kinematic model of fish pectoral fin. On the other hand, rigid fin rays are used to take the place of flexible fin rays which can realize active or passive deformation. Therefore, in order to improve the performance of the flexible bionic pectoral fin, it is necessary to develop the research on the design of the bionic pectoral fin and the establishment of the kinematic model of real fish pectoral fin.

VII. CONCLUSIONS

Based on the anatomy structure and neuromuscular control mechanism of fish pectoral fin, a new under-actuated flexible bionic pectoral fin was designed. Then, the kinematic and dynamic models of bionic pectoral fin were built. Finally, the performance of the bionic pectoral fin was analyzed during fish forward steady swimming by simulation. According to the analysis, the following conclusions can be got.

(1)Taking advantage of under-actuated technology, the new bionic pectoral fin reduces the number of the driving variables, providing the basis of reducing the volume as well as the complexity of bionic pectoral fin.

(2) The bionic pectoral fin can imitate the propulsion locomotion during fish forward steady swimming well. However, due to the restriction of kinematic model of pectoral fin and structure as well as physical properties of bionic fin ray, there is still tolerance between the locomotion morphology of bionic pectoral fin and that of real fish. Therefore, it is necessary to develop further research on kinematic modeling of pectoral fin and bionic design of fin ray.

(3) Based on the theoretical analysis, the new bionic pectoral fin can imitate all kinds of maneuvering motion morphology of pectoral fin besides the propulsion morphology during fish forward steady swimming, but the feasibility still needs to be validated further by simulation and experiment.

REFERENCES

[1] Michael Sfakiotakis, David M. Lane and J. Bruce C. Davies. Review of fish swimming modes for aquatic locomotion [J]. IEEE Journal of Oceanic Engineering, 1999, 24(2), pp.237-252

[2] F. E. Fish, G. V. Lauder and R. Mittal etc. Conceptual design for the construction of a biorobotic AUV based on biological hydrodynamics[C]. International Symposium on Unmanned Untethered Submersible Technology, New Hampshire, USA, 2003, pp.1-8

[3] George V.Lauder, Erik J. Anderson and James Tangorra, Fish biorobotics: kinematics and hydrodynamics of self-propulsion [J]. The Journal of Experimental Biology 210, 2009, pp.2767-2780

[4] G. V. Lauder and Peter G. A. Madden. Fish locomotion: kinematics and hydrodynamics of flexible foil-like fins[J]. Experiments in Fluids, 2009, 43(5), pp.641-653

[5] G. V. Lauder and E. G. Drucker. Morphology and experimental hydrodynamics of fish fin control surfaces[J]. IEEE Jounal of Oceanic Engineering, 2004, 29(3), pp.556-571

[6] G. V. Lauder, Peter G. A. Madden and R. Mittal etc. Locomotion with flexible propulsors: I. experimental analysis of pectoral fin swimming in Sunfish[J]. Bioinsp. Biomim.1(2006), S35-S41

[7] M. W. Westneat, D. H. Thorsen and J. A. Walker etc. Structure, function, and neural control of pectoral fins in fishes[J]. IEEE Jounal of Oceanic Engineering, 2004, 29(3), pp.674-683

[8] E. G. Drucker and J. S. Jensen. Kinematic and electromyographic analysis of steady pectoral fin swimming in the Surfperches[J]. The Jounal of Experimental Biology 200, 1997, pp.1709-1723

[9] S. Alben, Peter G. Madden and G. V. Lauder. The mechanics of active fin-shape control in ray-finned fishes[J]. J. R. Soc. Interface, 2010(4), pp.243-256

[10] J. Palmisano, R. Ramamurti and K. J. Lu etc. Design of a biomimetic controlled-curvature robotic pectoral fin[C]. IEEE International Conference on Robotics and Automation, Italy, 2009, pp. 966-973

[11] R. Ramamurti, J. Geder, J. Palmisano etc. Computations of Flapping Flow Propulsion for UUV Design[C]. 47th AIAA Aerospace Sciences Meeting Including the New Horizons Forum and Aerospace Exposition, Orlando, Florida , 2009-752, pp.1-33

[12] J. L. Tangorra, S. N. Davidson and I. Hunter etc. The development of a biologically inspired propulsor for unmanned underwater vechicles[J]. IEEE Journal of Oceanic Engineering, 2010, 32(3), pp.533-550

[13] J. R. Gottlieb. The development of a multi-functional bio-robotic pectoral fin[D]. Drexel University, 2010

[14] James L. Tangorra, George V. Lauder Ian W. Hunter etc. The effect of fin ray flexural rigidity on the propulsive forces generated by a biorobotic fish pectoral fin[J]. The Journal of Experimental Biology 213, 2010, pp.4043-4054

[15] Dean H. Thorsen and Mark W. Westneat. Diversity of pectoral fin structure and function in fishes with labriform propulsion[J]. Journal of Morphology, 2005, 263(2): pp.133-150

[16] Kourosh Shoele and Qiang Zhu. Numerical simulation of a pectoral fin during labriform swimming[J]. The Journal of Experimental Biology 213, 2010, pp.2038-2047

[17] Xie Haibin. Design, modeling, and control of bionic underwater vehicle propelled by multiple undulatory fins [D]. National University of Defense Technology, 2006

[18] Zhang Daibing, Research on the Underwater Bionic Undulatory-Fin Propulsor and Its Control Method[D].National University of Defense Technology, 2009

[19] Constantinou M. C., Symans M. D., Experimental and Analytical Investigation of Seismic Response of Structure with Supplement Fluid Viscous Damper, Report-92-0032 [R]. NCEER, 1992

Qiang Liu ShanDong Province, China. Birthdate: March, 1980. is Control Theory and Control Engineering Ph.D., graduated from School of Automation Harbin Engineering University. And research interests on underwater vehicles.

He is a senior lecturer of School of Electronic Engineering, Huaihai Institute of Technology.